Compression Behavior of Langmuir−Blodgett Monolayers of Regioselectively Substituted Cellulose Ethers with Long Alkyl Side Chains

Wakako Kasai,[†,‡] Shigenori Kuga,[†] Jun Magoshi,[§] and Tetsuo Kondo*[,||]

Graduate School of Agricultural and Life Sciences, The University of Tokyo, Yayoi 1-1-1, Bunkyo-ku, Tokyo 113-8657, Japan, National Institute of Agrobiological Resources (NIAR), 2-1-2 Kannondai, Tsukuba, Ibaraki 305-8602, Japan, and Graduate School of Bioresource and Bioenvironmental Sciences, Kyushu University, 6-10-1, Hakozaki, Fukuoka, 812-8581, Japan

Received November 1, 2004. In Final Form: December 26, 2004

Regioselectively substituted alkylcellulose ethers having long alkyl side chains, 6-*O*- (6C18), 2,3-di-*O*- (23C18), and tri-*O*-octadecyl-cellulose (triC18) were successfully synthesized. The key step of these syntheses was removal of the residual alkylation reagent by an isothermal crystallization procedure to isolate and purify the compounds, since a physical entanglement between the long alkyl side chains in the cellulose derivatives and the reagent had caused difficulty in obtaining the purified derivatives. After the monolayers from these cellulose ethers were fabricated on a water surface, they were deposited on substrates by a vertical dipping method to be Langmuir−Blodgett (LB) monolayers. During the compression process of each monolayer, a surface pressure (π)−area (A) isotherm behaved in a different way. Atomic force microscopy (AFM) was employed to interpret changes of the surface topography of the obtained LB monolayers depending on the surface pressure. The compressed 23C18 LB monolayer was observed to be more homogeneous than other samples. On the basis of the LB monolayer thickness estimated by AFM as well as X-ray reflection measurements, the 23C18 LB monolayer was assumed to possibly possess the vertical arrangement of an up-ordering of all the alkyl side chains on the individual glucose ring against the water surface. In other words, with increase in the surface pressure, the usual conformation of a 2_1 screw of cellulose backbone may be changed into an unusual conformation with a certain $\phi-\psi$ dihedral angle resulting in 1-fold axis without a symmetry element. These results suggest that the formation of such compressed LB monolayers was strongly influenced by the hydrophobic interaction among the distribution of the long alkyl side chains in the anhydroglucose unit and further lack of inter- and/or intramolecular hydrogen bonds engaged in cellulose ethers, and as a result, those effects may even change the main chain conformation.

1. Introduction

Ordered monolayer films transferred from a water surface onto a solid substrate by the Langmuir−Blodgett (LB) technique provide growing application in various fields such as microelectronics, sensors, and biomimetic membranes. This is because such LB films have a great possibility to artificially organize molecular assemblies with desired structures and properties in atomic scale and nanoscale. To date, some attempts at the preparation and characterization of LB films of cellulose derivatives have been made. Cellulose, which is a β-1,4-linked glucan homopolymer, is one of the most abundant and also sustainable natural resources on the earth. Creation of new functional materials would be possible from this natural resource if the cellulose suprastructure can be controlled at the nanoscale using the LB technique. The spreading behavior of cellulose acetate and *O*-ethylcellulose on a water surface at the air−water interface was investigated more than 60 years ago.[1−4] Monolayers of cellulose derivatives as a material were, however, not transferred on substrates until Kawaguchi et al. succeeded in preparing multilayers of cellulose esters by the horizontal lifting method.[5] Since then, LB monolayers of cellulose ethers have been extensively studied with respect to properties as LB films.[6−9] Among them there were only a few reports about the fine surface structure and thickness of LB monolayers.[10,11] Considering *O*-alkylcellulose derivatives as polymer substrates, it has not been investigated that distribution of alkyl side chains may have an effect on monolayer morphology, although the relationship between surface morphology and length of alkyl side chains has been investigated.[5,8,10] Since physical properties of monolayers are generally correlated with the fine structure including the super- and supramolecular structures, it is of importance to investigate the detailed information of the LB monolayer structures.

Various techniques are used for understanding fine structures of monolayers. The main tools are polarized Fourier transform infrared spectroscopy (FT-IR) and X-ray and electron diffraction,[8,9,12,13] but they provide only

* Corresponding author: tekondo@agr.kyushu-u.ac.jp.
† The University of Tokyo.
‡ Present address: Graduate School of Bioresource and Bioenvironmental Sciences, Kyushu University, 6-10-1, Hakozaki, Fukuoka, 812-8581, Japan.
§ National Institute of Agrobiological Resources.
|| Kyushu University.

(1) Katz, J. R., Samwel, P. J. P., *Naturwissenschaften* **1928**, *16*, 592.
(2) Adams, N. K. *Trans. Faraday Soc.* **1933**, *29*, 90.
(3) Borgin, K.; Johnson, P. *Trans. Faraday Soc.* **1953**, *49*, 956.
(4) Giles, C. H.; Agnihotri, V. G. *Chem. Ind.* **1967**, *4*, 1874.
(5) Kawaguchi, T.; Nakahara, H.; Fukuda, K. *Thin Solid Films* **1985**, *133*, 29.
(6) Basque, P.; Gunzbourg, A.; Rondeau, P.; Ritcey, A. M. *Langmuir* **1996**, *12*, 5614.
(7) Fischer, P.; Brooks, C. F.; Fuller, G. G.; Ritcey, A. M.; Xiao, Y.; Rahem, T.; *Langmuir* **2000**, *16*, 726.
(8) Mao, L.; Ritcey, A. M. *Langmuir* **1996**, *12*, 4754.
(9) Schaub, M.; Fakirov, C.; Schmidt, A.; Lieser, G.; Wenz, G.; Wegner, G.; Albouy, P.-A.; Wu, H.; Foster, M. D.; Majrkzak, C.; Satija, S. *Macromolecules* **1995**, *28*, 5614.
(10) Ito, T.; Tsujii, Y.; Suzuki, H.; Fukuda, T.; Miyamoto, T. *Polym. J.* **1992**, *24*, 641.
(11) Kimura, S.; Kusano, H.; Kitagawa, M.; Kobayashi, H. *Appl. Surf. Sci.* **1999**, *142*, 585.
(12) Kimura, F.; Umemura, J.; Takenaka, T. *Langmuir* **1986**, *2*, 96.

10.1021/la047323j CCC: $30.25
Published on Web 02/15/2005

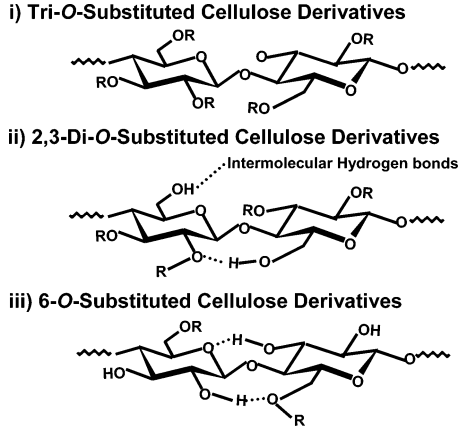

Figure 1. Chemical structures and possible hydrogen bonds in regioselectively substituted cellulose ethers. The doted lines indicate hydrogen bonds.

indirect information on monolayer structures. On the other hand, it is becoming possible to observe fine structures of a film surface using transmission electron microscopy (TEM) and atomic force microscopy (AFM). Miyamoto et al. examined the LB monolayer structure of a cellulose tri(*n*-decanoate) and cellulose tri(*n*-octadecanoate) having a long side chain by TEM.[10] AFM, which is capable of visualizing surface structures at the molecular scales in the air, is a facile and convenient method when compared with TEM in the light of sample preparation. Thus, AFM is presently the best tool to elucidate the fine structure on the surface of organic materials.

In this article, we will describe at first syntheses of regioselectively substituted cellulose ethers, 6-*O*- (6C18), 2,3-di-*O*- (23C18), and tri-*O*-octadecylcellulose (triC18), and the subsequent preparation of the LB monolayer films of these cellulose ethers under desired compression conditions by a vertical lifting method on the water surface. The structure and thickness of the LB monolayers were investigated using AFM and X-ray reflection. Distribution of substituents within the anhydroglucose units as well as along the chain in cellulose derivatives is believed to influence strongly physical properties such as solubility and crystallization.[14] Thus, a goal of the present study is to clarify how distribution of the substituent within an anhydroglucose unit contributes to self-assembly of molecules in a compression process of the monolayers as LB films. Change of the arrangement of the molecular chains in the LB monolayers during the compression was also investigated.

2. Experimental Section

2.1. Sample Preparation. 2.1.1. Preparation of Tri-*O*-octadecylcellulose (triC18). Figure 1 illustrates the chemical structure of regioselectively substituted cellulose ethers synthesized here including possible hydrogen bonding formation under a stress-free condition.[14]

The alkylation procedure was basically according to the method of Kondo and Gray.[15] Commercial cellulose acetate from cotton linters with degree of polymerization (DP) about 200 and degree of substituents (DS) about 2.24 provided by Daicel Chemical Ind. Co., Ltd. was the starting material. The sample was dried at 105 °C for 3 h. Dimethyl sulfoxide (DMSO) was dehydrated over type 3A molecular sieves. Reagent-grade solvents and alkylating agents (Aldrich Gold Label) were used without further purification. Powdered sodium hydroxide was pulverized by grinding NaOH pellets in a domestic coffee mill. At first, cellulose acetate (1.0 g) was completely dissolved in 60 mL of DMSO at 60 °C for 1 h with a constant stirring and then 1 mL of water was added. A 5.9 g portion of NaOH was dispersed in this CA−DMSO solution containing 1 mL of water. Following 1 h of stirring under a nitrogen atmosphere, two-thirds of the total amount of the octadecyl bromide (40.7 g)/10 mL of DMSO was added dropwise to the solution. At 2, 3, and 4 h after the first addition of the octadecyl bromide, one-third of the remaining octadecyl bromide (13.6 g)/10 mL of DMSO was added dropwise, respectively. Following the last addition of the octadecyl bromide in DMSO to the solution, the temperature was raised to 70 °C and kept at this temperature for 20 h under a nitrogen atmosphere. The reaction mixture was cooled to room temperature, and then 100 mL of both water and methylene chloride was added. The methylene chloride layer was separated, washed with water twice, and evaporated under a reduced pressure at 40 °C until a syrup remained. The product was precipitated from the syrup by the addition of 100 mL of methanol. Following filtration, the precipitate was again dissolved in methylene chloride. The solution was cooled at 5 °C and kept there for 12 h. The excess alkylation reagent was precipitated in methylene chloride by the isothermal crystallization at such a low temperature, whereas the obtained cellulose derivatives were still dissolved in the solvent. In this way, the residual octadecyl bromide can be removed by centrifugation kept at the low temperature. To purify cellulose ethers thus prepared, the procedure was repeated more than five times. The obtained solution was poured into ethanol to yield the product as a precipitate, and the product was filtered and dried under vacuum at 40 °C.

2.1.2. Preparation of 2,3-Di-*O*-octadecylcellulose (23C18). 2,3-Di-*O*-octadecylcellulose (23C18) was prepared from 6-*O*-triphenylmethylcellulose (Tritylcellulose) with DP 180 as the starting material by a modified procedure of Kondo and Gray.[16] Tritylcellulose (1.0 g) was dissolved completely in 60 mL of DMSO at 60 °C for 1 h with a constant stirring. 2.5 g of powdered NaOH was dispersed in the solution containing 1 mL water. Following 1 h of stirring under a nitrogen atmosphere, two-thirds of the total amount of the octadecyl bromide (17.2 mg) /10 mL DMSO was added dropwise to the solution. At 2,3 and 4 h after the first addition of the octadecyl bromide, one-third of the remaining octadecyl bromide (5.73 mg)/10 mL DMSO was added dropwise, respectively. Following the last addition of the octadecyl bromide to the solution, the temperature was raised to 70 °C and kept there for 20 h under the nitrogen atmosphere. The mixture was cooled to room temperature and the product was isolated and purified as described above. The purified product (4.5 g) was then detritylated with hydrogen chloride gas bubbling for 4 min in the 150 mL of methylene chloride solution.[17] The detritylated mixture was poured into 300 mL of acetone to have a detritylated product as a precipitation. The detritylated product was isolated by centrifugation, washed with acetone, filtered and dried under vacuum at 65 °C.

2.1.3. Preparation of 6-*O*-Octadecylcellulose (6C18). 6-*O*-Octadecylcellulose (6C18) was prepared also from tritylcellulose with DP 180 as the starting material by the modified procedure of Kondo.[18] In the procedure, the 2,3-di-*O*-(1-propenyl)cellulose was obtained following the previous paper.[18] Basically, the alkylating procedure for OH group at the C-6 positions was the same as that employed for 23C18. The synthesized 2,3-di-*O*-(1-propenyl)cellulose (1.5 g) was completely dissolved in DMSO (90 mL). Powdered NaOH (3.1 g) was dispersed in the solution containing 1.5 mL of water. After 1 h of stirring under a nitrogen atmosphere, two-thirds of the total amount of the octadecyl bromide (21.6 mg)/10 mL of DMSO was added dropwise to the solution. At 2, 3, and 4 h after the first addition of the octadecyl bromide, one-third of the remaining octadecyl bromide (7.2 mg)/10 mL of DMSO was added dropwise, respectively. Following the last addition of octadecyl bromide, the solution was kept under a nitrogen atmosphere for 20 h at 70 °C. As described in section 2.1.2., the isolation, purification, and detritylation following this reaction were accomplished. 1-Propenyl groups in

(13) Kajiyama, T.; Umemura, K.; Uchida, M.; Oishi, Y.; Takei, R. *Bull. Chem. Soc. Jpn*. **1989**, *62*, 3004.
(14) Kondo, T. *J. Polym. Sci., Part B*: *Polym. Phys.* **1997**, *35*, 717.
(15) Kondo, T.; Gray, D. G. *J. Appl. Polym. Sci.* **1992**, *45*, 417.
(16) Kondo, T.; Gray, D. G. *Carbohydr. Res.* **1991**, *220*, 173.
(17) Horton, D.; Just, E. K. *Carbohydr. Res*. **1973**, *30*, 349.
(18) Kondo, T. *Carbohydr. Res.***1993**, *238*, 231.

the obtained 6-*O*-octadecyl-2,3-di-*O*-(1-propenyl) cellulose was then removed to provide 6-*O*-octadecylcellulose by the method given in a previous paper.[18]

2.2. Analyses. During the reaction processes, the compounds were confirmed by IR measurements and solution ^{13}C NMR. IR spectra were obtained using a JASCO FT/IR-620 with a TGS detector at room temperature. Sixteen scans were averaged with a resolution of 2 cm^{-1}. The wavenumber region investigated ranged from 4000 to 400 cm^{-1}. ^{13}C NMR spectra were obtained with a Varian XL 200 spectrometer operating at 50.4 MHz, on samples dissolved in deuterated chloroform ($CDCl_3$), DMSO (DMSO-d_6), and pyridine-d_5 (C_5D_5N). Chemical shifts were measured from the solvent signals (δ_c 77.01 ppm for $CDCl_3$, δ_c 149.9, 135.5, 123.5 ppm for C_5D_5N, and δ_c 39.6 ppm for DMSO-d_6) from internal tetramethylsilane, respectively. The pulse delay was set as 0.5 s and 5000 times accumulation was used.

For the confirmation of the final products, cross polarization magic angle spinning (CP/MAS) ^{13}C NMR spectra were obtained by Chemagnetics CMX-300 spectrometer operating at resonance frequencies of 75.57 MHz for ^{13}C with a CP/MAS at room temperature. Cross polarization times typically were 1−2 ms. The recycle time of the pulse sequence was 10 s. The spectra were accumulated ca. 500 times. The chemical shift (29.47 ppm from $(CH_3)_4Si$) of the CH for adamantane crystals was used as an external reference to determine chemical shifts.

2.3. Preparation of the LB Monolayer. Monolayers were characterized at the air−water interface using NL-BIO40-MWCT (Laser Techno Co., Ltd.). The cellulose ethers were dissolved in methylene chloride (0.05% (w/v) 10−15 μL) to provide a clear solution. The individual solutions were spread on a clean water surface in a Teflon-coated trough (40 × 200 mm^2). The subphase superpure water was purified by the Milli Q-II system (Millipore Co., Ltd.). Compression of the surface areas by the moving Teflon-coated barrier was started 30 min after the drop of the sample when evaporation of the solvent was completed on the water surface. The compression rate was 20 mm/min, and the surface pressure was recorded by the Wilhelmy method.[20] For observation of the surface morphology using AFM, LB monolayers of 6C18, 23C18, and triC18 were prepared at various surface pressures as shown in Figure 8 by a vertical dipping method. For film thickness measurements using AFM and X-ray diffraction, the LB monolayers of 23C18 prepared at a surface pressure of 7.5 mN/m were employed.

2.4. Observation of the Surface Structure and Measurements Thickness of LB Monolayers Using AFM. The monolayer on the water surface was deposited on mica substrates by a vertical lifting method for observing the surface structure using AFM. A Nanoscope IIIa (Digital Instruments Co.) microscope was employed and performed in air at room temperature, being controlled in tapping mode with a scan rate from 1 to 5 to observe from 10 to 1 μm^2. The AFM tip was a commercial silicon tip with a nominal radius from 5 to 10 nm, which was mounted on a rectangular cantilever with a spring constant of about 46 N/m (NCH). The scanning was carried out along the compressed direction of the monolayer. For measuring the LB monolayer thickness, the monolayer on a mica substrate was dipped into methylene chloride to remove the disordered regions of the surface structure. Then the height of the remaining well-ordered regions in the LB monolayer after dipping was measured based on the mica surface estimated as 0 value. The dipping time was set from 0 to 3 h.

2.5. Evaluation of the LB Monolayer Thickness Using the X-ray Diffraction. X-ray diffraction pattern was recorded by the X-ray reflective technique using a Rigaku ATX-E. The measurements of reflective curves were performed using a coupled $\theta/2\theta$ scan. The X-ray source is a rotation target tube with a copper anode. Cu Kα radiation from a copper rotating anode was filtered to use for the experiment. The experiments presented were performed with a generator setting of 50 kV/300 mA. The X-ray beam was concentrated by an X-ray mirror system. Incident angles (ω) for out-of-plane measurement were between 0 and 5°. Each LB monolayer was transferred on a microscope slide for the X-ray measurement. The $\theta/2\theta$ was obtained on the monolayer in the above optical system, and the film thickness was estimated by a simulation method of nonlinear least-squares fitting of the measured data profile with the calculated profile based on the theoretical formula according to the procedure of Hirano et al.[21−24]

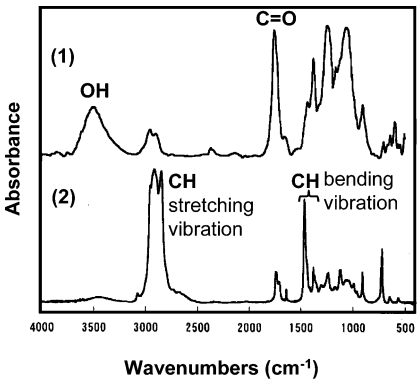

Figure 2. Change of IR spectra toward triC18: (1) cellulose acetate and (2) tri-*O*-octadecylcellulose (triC 18).

3. Results and Discussion

3.1. Preparation and Characterization of Regioselectively Substituted Cellulose Ethers. 3.1.1. Change of IR Spectra during the Preparation. 3.1.1.1. Tri-*O*-octadecylcellulose (triC18). Figure 2 shows IR spectra of cellulose acetate (1) and the alkylated product of the cellulose acetate (2). Following the alkylation, the amounts of remaining acetyl groups in the treated sample were almost negligible. The OH stretching vibration at 3400 cm^{-1} disappeared. The alkylated compound from cellulose acetate had strong absorption peaks around 2800−3000 cm^{-1} and 1460 and 1370 cm^{-1}, due to C−H stretching and C−H bending vibrations, respectively. This means that the three hydroxyl groups as well as acetyl groups in an anhydroglucose residue were almost completely substituted by the alkyl groups, indicating preparation of tri-*O*-cellulose alkyl ether.

3.1.1.2. 2,3-Di-*O*-octadecylcellulose (23C18). Figure 3 shows IR spectra of starting material, tritylcellulose (1), the alkylated tritylcellulose (2), and detritylated sample after the alkylation (3). The OH stretching vibration at 3400 cm^{-1} almost completely disappeared with alkylation of tritylcellulose (Figure 3(2)). This indicates that hydroxyl groups at the C-2 and C-3 positions were regioselectively substituted by the alkyl groups. The absorption bands at 1598, 1491, and 1499 cm^{-1} due to the trityl group disappeared after detritylation with hydrogen chloride gas bubbling as shown in Figure 3(3). This suggests that the hydrogen chloride gas treatment successfully removed the trityl groups. It should be added that because of the strong intensity due to the alkyl group, OH groups were apparently very small in the normalized spectrum (3). Instead, the CP/MAS ^{13}C NMR spectrum clearly identified the compound as described later.

(19) Kondo, T.; Isogai, A.; Ishizu, A.; Nakano, J. *J. Appl. Polym. Sci.* **1987**, *34*, 55.

(20) Roberts, G. *Langmuir−Blodgett Films*; Plenum Press: New York and London, 1990; p 106.

(21) Kimura, S.; Kitagawa, M.; Kusano, H.; Kobayashi, H. *Novel Method to Study Interfacial Layers*; Möbius, D., Miller, R., Eds.; Elsevier Science: Amesterdam, 2001; pp 255−264.

(22) Hirano, T.; Matsuo, R.; Tomiyama, K.; Yazawa, I.; Wada, H.; Otaki, M., Omote, K. *19th Annual Bacus Symposium on Photomask Technology and Management*: *15−17 September 1999 Monterey, California*; Abboud, F. E., Grenon, B. J., Eds.; SPIE Proceedings Series Volume 3873; International Society for Optical Engineering: Bellingham, WA, 1999; p 562.

(23) Parrat, L. G. *Phy. Rev. B* **1954**, *95*, 359.

(24) Shinha, S. K.; Sirota, E. B.; Garoff, S.; Stanley, H. B.*Phy. Rev. B* **1988**, *38*, 2297.

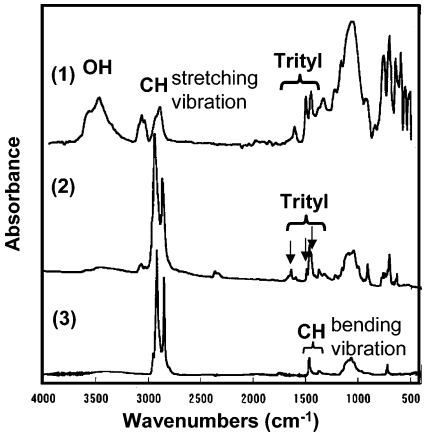

Figure 3. Change of IR spectra depending the process toward 23C18: (1) tritylcellulose, (2) 2,3-di-*O*-octadeyl-6-*O*-tricellulose, and (3) 2,3-di-*O*-octadecylcellulose (23C18).

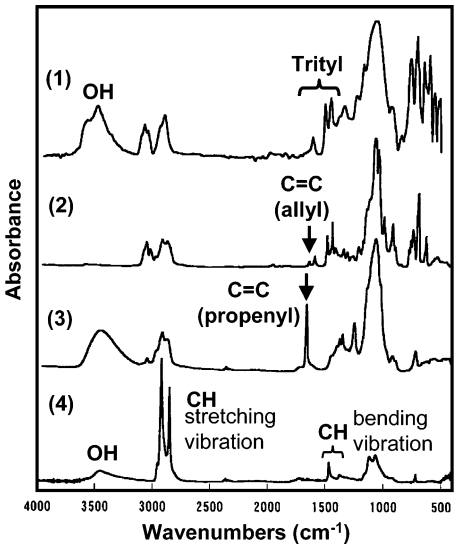

Figure 4. Change of IR spectra depending the process toward 6C18: (1) tritylcellulose, (2) 2,3-di-*O*-allyl-6-tritylcellulose, (3) 2,3-di-*O*-(1-propenyl)cellulose, and (4) 6-*O*-octadecylcellulose (6C18).

3.1.1.3. 6-*O*-Octadecylcellulose (6C18). Figure 4 shows change of IR spectra of intermediate compounds from tritylcellulose (1) to 6-*O*-octadecylcellulose (4). First, the OH groups in the tritylcellulose were completely allylated (2). By the allylation, the OH stretching vibration around 3400 cm^{-1} disappeared, while C=C absorption bands due to the allyl double bonds appeared around 1647 cm^{-1}, indicating 2,3-di-*O*-allyl-6-*O*-tritylcellulose (Figure 4(2)). The 2,3-di-*O*-allyl-6-*O*-tritylcellulose was then treated with hydrogen chloride gas to remove the trityl groups. The absorption bands at 1598, 1491, and 1499 cm^{-1} due to the trityl group disappeared, whereas the OH stretching vibration around 3400 cm^{-1} appeared because of completion of removal of the trityl groups. Then the allyl ether was isomerized[18,25] to the *cis*-1-propenyl group (Figure 4(3)). The prototropic rearrangement of the allyl ether group to their propenyl analogues was performed effected by employing potassium *tert*-butoxide. During the reaction, the absorption band at 1647 cm^{-1} due to allyl double bonds ($-OCH_2CH{=}CH_2$) decreased as a function of the reaction time, being replaced by the new band at 1669 cm^{-1} due to 1-propenyl double bonds ($-O-CH{=}CH-CH_3$) as shown in Figure 4(3).

(25) Prosser, T. J. *J. Am. Chem. Soc.* **1961**, *83*, 1701.

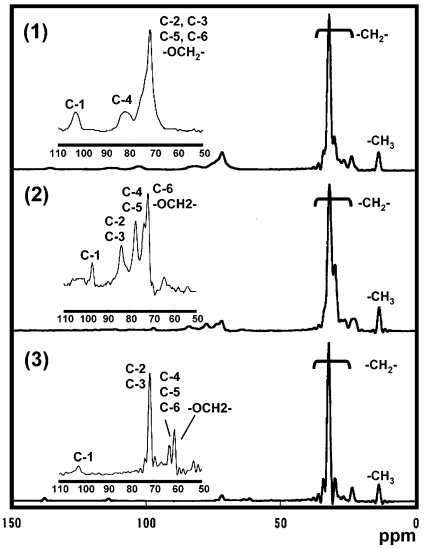

Figure 5. CP/MAS ^{13}C NMR spectra in the range between 0 and 150 ppm and between 50 and 110 ppm for (1) 6C18, (2) 23C18, and (3) triC18.

Figure 4(4) shows the IR spectra of the obtained 6-*O*-octadecylcellulose. By the deblocking reaction, the absorption bands 1669 cm^{-1} due to 1-propenyl double bonds disappeared, and instead, the CH stretching and bending vibration due to the octadecyl side chains appeared strongly. The OH stretching vibration around 3400 cm^{-1} also appeared.

3.1.2. CP/MAS ^{13}C NMR Confirmation for the Products. To confirm the chemical structure of the obtained regioselectively substituted *O*-alkylcelluloses, the CP/MAS ^{13}C NMR spectra were employed (Figure 5). The signals appearing around 14 ppm were assigned to methyl carbon of the octadecyl substituents. The signal for the methylene carbons in the octadecyl substituents was located around 20−40 ppm. The signals from C-2 to C-6 position appeared around 60−90 ppm, whereas the signal at 100 ppm was assigned to the C-1 position. Chemical shifts of carbon signals were slightly different among the three cellulose samples because they were influenced by distribution of the alkyl groups. In general, the signals of carbon atoms exhibit a downfield shift of ca. 10 ppm by etherification and a number of upfield shifts by an adjacent effect.[26] With the three spectra, the three regioselectively substituted octadecyl celluloses were all identified.

It should be noted that the key step of these syntheses was removal of the residual C18 alkylation reagent in the purification step, because strong physical entanglements between side chains in the cellulose derivatives and the residual alkylation reagent made the purification hard.[27] In this study, the residual reagent was possibly removed by the isothermal crystallization as the manner described in the Experimental Section. Significant depolymerization of all products did not occur during the alkylation, based on the result of size-exclusion chromatograms (data not shown). Therefore, it is indicated that DP of all the cellulose samples thus prepared should have almost the same value of starting materials; triC18 with DP200, 23C18 with DP180, and 6C18 with DP 180.

3.2. Characterization of Compressed LB Monolayers of the Cellulose Ethers. 3.2.1. Molecular Chain Arrangements Based on the $\pi-A$ Isotherms of Cellulose Ethers. Figure 6 shows $\pi-A$ isotherms of 6C18,

(26) Kondo, T. *J. Polym. Sci., Part B*: *Polym. Phys.* **1994**. *32*. 1229.
(27) Isogai, A.; Ishizu, A.; Nakano, J. *J. Appl. Polym. Sci.* **1986**, *31*, 341.

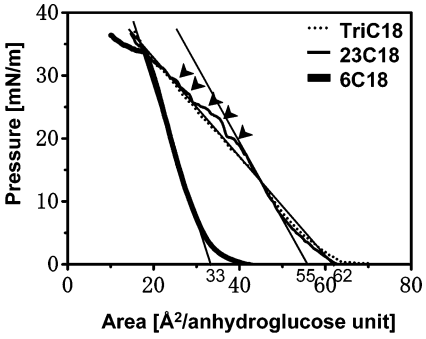

Figure 6. $\pi-A$ isotherm of triC18, 23C18, and 6C18 spread from dichloromethane solution at 298 K. (Black arrows indicate critical point of 23C18.)

23C18, and triC18 (these abbreviations correspond to the above monolayers that were prepared from methylene chloride solutions at 298 K). The surface pressure of 6C18 increased drastically with decreasing of the area at 40 Å^2 per anhydroglucose unit. When the surface pressure increased further with compression, collapse of the monolayer was observed at 20 Å^2 per anhydroglucose unit. On the other hand, in the $\pi-A$ isotherms of 23C18 and triC18, the surface pressures began to increase at almost same position of about 70 Å^2 per anhydroglucose unit with decrease in the area due to the compression. However, details of the two isotherms behaved in a different fashion. The 23C18 started to exhibit a fluctuation of the isotherm above 18 mN/m as indicated by arrows in Figure 6, which is ascribed to collapse of the monolayer as could be seen in the AFM image of Figure 8f. In the triC18 monolayer such a fluctuation was not provided. This indicates that the formation behavior of the monolayers in triC18 and 23C18 may be different depending on the regioselectivity of alkyl side chains within anhydroglucose unit. Limiting molecular areas per anhydroglucose unit obtained by extrapolation to zero surface pressure were about 33, 55, and 62 Å^2 for 6C18, 23C18, and triC18 monolayers, respectively. Basque et al. reported that the $\pi-A$ isotherms of the cellulose triethers with a series of alkyl side chains having relatively medium length had a trend of decrease in the limiting molecular areas per anhydroglucose unit from 113 to 60 Å^2 with decrease in length of the alkyl side chains from dodecyl (C12) to butyl (C4), indicating formation of a characteristic liquid analogous phase with a plateau area. In this report, however, limiting molecular areas of the regioselectively substituted cellulose ethers with the long alkyl side chains of C18 were small when compared with their samples. Moreover, the $\pi-A$ isotherm of our samples did not imply such a plateau area as shown Figure 6, as is the same for stearic acid and cellulose tri-(*n*-octadecanoate).[10] This indicates that such a formation of liquid analogous phase on the monolayer formation may be dependent on the length of alkyl side chains. This is presumably because alkyl side chains with a short or medium length do not have enough hydrophobicity to stick up against the water surface, resulting in longer limiting molecular area than that for cellulose ethers having longer side chains. This means that the shorter alkyl side chains still spread over water phase even after compression.

Considering molecular arrangements of these cellulose ethers as a monolayer form, it is assumed that two kinds of molecular arrangements can be assumed depending on the distribution of the long alkyl group, as shown in Figure 7. One is the parallel arrangement of glucose ring planes over the water surface as shown in Figure 7A. The other is the vertical arrangement of the planes with facing each glucose ring over the water surface (Figure 7B). Arrangement of glucose ring planes is assumed by estimating the values of the limiting molecular area. Then, it is indicated that the monolayers of triC18 were composed in the parallel arrangements as shown in Figure 7A, whereas that of 6C18 owned the vertical arrangement as shown Figure 7B. The case of 23C18 will be discussed later separately in section 3.2.4.

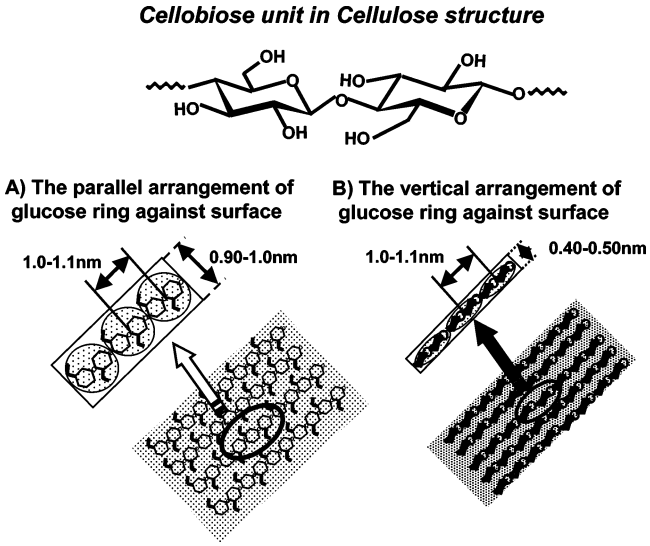

Figure 7. Schematic images of the arrangement of glucose ring planes on the water surface.

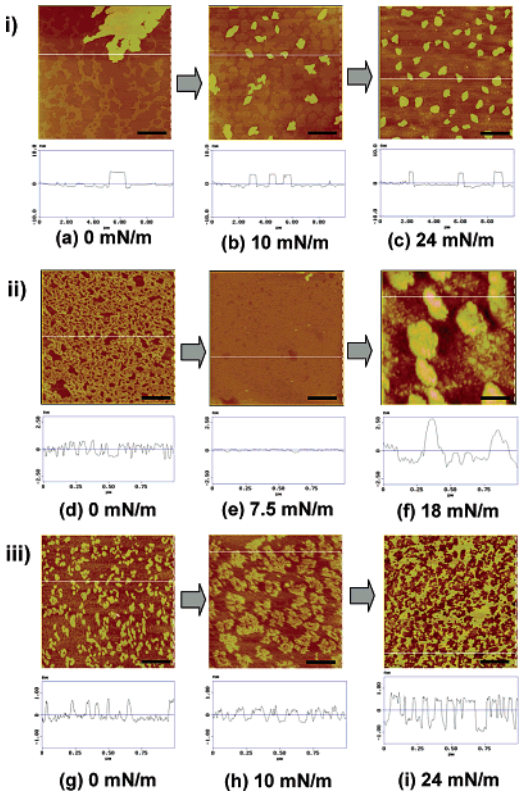

Figure 8. Dependence of the target pressure on the LB monolayer surface topography in the $\pi-A$ isotherms as shown in Figure 6: (i) triC18, (ii) 23C18, and (iii) 6C18. Scale bar: (a–c) 2 μm, (d–i) 200 nm.

3.2.2. Behavior of the Molecular Assembly Resulting in Change of Topography of the LB Monolayers. Figure 8 showed surface topography and the cross section of the surface transferred at the various pressures for 23C18, 6C18, and triC18, respectively. The 23C18 LB monolayer could be most perfectly transferred to a mica

substrate of the three samples. However, LB monolayers of 6C18 and triC18 were not successfully transferred to mica despite the same preparing condition. The transfer ratios of 6C18 and triC18 were more than 1. This indicated that the structure of the 23C18 LB monolayer might be more stable than those of the other two LB monolayers. As the surface pressure of all samples increased with compression, the surface topography changed drastically. At the initial stage, large aggregates over 5 μm^2 were observed only in triC18 flat LB monolayers within 4 nm in roughness (Figure 8a). Then, the domain size of the structure became smaller gradually with increasing in the surface pressure. The long alkyl side chains of triC18 may form a pseudocrystal structure partially at the initial stage, because many long alkyl chain groups were stuck up against the water surface and thus aggregated by some strong hydrophobic interactions. Then, the brittle pseudocrystalline structure may collapse and get smaller with further increasing in the surface pressure. A network structure of 23C18 may be formed at the initial stage (Figure 8d) prior to the compression. As the compression proceeded to 7.5 mN/m (Figure 8e), a smooth surface was observed. This indicates that an apparently homogeneous film may be prepared by the compression of the initial network structure. In panel f of Figure 8, with further compression the LB monolayer may be partially or largely collapsed to form overlapped areas shown as some larger domains appearing in the AFM image. The LB monolayer of 6C18 was composed of small grains already at the initial monolayer phase (Figure 8g). Through all stages of the compression, domains of some periodic structures in 6C18 were observed in the cross section (Figure 8h,i). The LB monolayer of 6C18 has not collapsed, so obviously panel i of Figure 8 is a midway to the collapse. This indicates that the LB monolayer of 6C18 may not be homogeneous and more elastic than brittle when compared with that of triC18.

3.2.3. Thickness of the LB Monolayers Based on AFM and X-ray Reflection Measurements. The compressed LB monolayer of 23C18 shown in Figure 8e was chosen as an optimal homogeneous monolayer film. To measure the thickness of the film by AFM, it was soaked in a methylene chloride to remove disorder regions and thereby obtain only ordered regions remaining intact. In this way, a boundary between the ordered regions and the empty mica surface provided by the removal of the disordered region appeared clearly in the LB monolayer. Then, AFM tip could easily scan the selective area showing the height gap. First, change of the height depending on the soaking time was investigated because it was assumed that a maximum gap in height might occur between the perfectly ordered domain and the empty mica surface depending on the soaking time.

Namely, if the long alkyl chains stuck up over the water surface and thereby self-aggregated, they might form a pseudocrystalline structure similar to the polyethylene crystalline structure. When LB monolayers having such an ordered form were dipped in methylene chloride as a good solvent, the nonordered domains would be easily washed away and the obtained ordered domains that were more insoluble and stabilized could remain on the mica substrate. As shown in Figure 9, the optimal height of the remaining domains after dipping for 30 min was about 3.7 ± 0.2 nm in the 23C18. The height obtained at soaking times of 15, 45, and 60 min was between 2.5 and 3 nm. It is indicated that disorder regions of the LB monolayer surface started to be dissolved during the first 15 min, and then the rest of the disordered domains were completely removed after 30 min. When soaked over 30 min, the ordered domains started to be dissolved. It is considered that soaking in methylene chloride may affect the molecular orientation of so-called ordered monolayer domains. The domains in the 23C18 LB monolayer were not dissolved completely in methylene chloride even after 3 h. On the contrary, the domains in the 6C18 LB monolayer disappeared on the mica substrate over 30 min of dipping (data not shown). This agrees with the previous report that 6-*O*-substituted cellulose derivatives exhibit excellent solubility due to a lack of intermolecular hydrogen bonds.[14] The LB monolayer of triC18 was much easier to be dissolved by methylene chloride, because of high solubility of the monolayer of triC18 due to lack of the intra- and intermolecular hydrogen bonds as shown in Figure 1. An X-ray reflectivity profile obtained for the compressed LB monolayer from 23C18 shown in Figure 8e is presented in Figure 10. In this measurement, the LB monolayer thickness was estimated from the so-called Kiessig fringe,[28] and it was found to be 3.60 nm in thickness for this 23C18 LB monolayer. This value has good agreement with the value of 3.7 ± 0.2 nm obtained by the AFM measurements as described above. Thus, it is verified that the thickness of the LB monolayer could be also estimated using the AFM method.

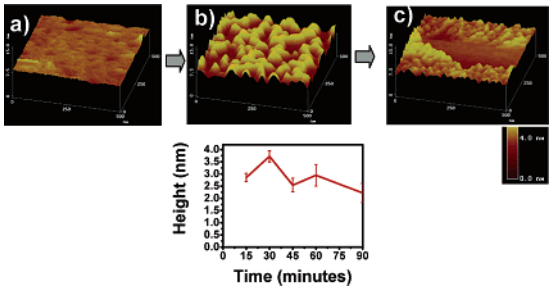

Figure 9. Dependence of the LB monolayer structure and height on the soaking time in dichloromethane solution after 23C18 (Figure 8f): (a) 0 min, (b) 30 min, and (c) 60 min.

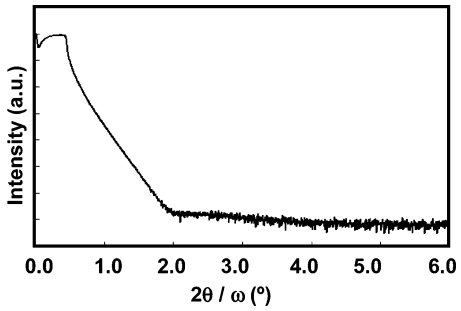

Figure 10. X-ray reflectivity profile of 23C18 LB monolayer.

3.2.4. Side Chain Arrangements Based on the Estimated Thickness of the LB Monolayer Film. As mentioned in section 3.2.1., the arrangement of glucose ring planes over the water surface can be two alternative forms, the parallel arrangement (Figure 7A) and the vertical arrangement (Figure 7B) of the glucose ring planes. When the alkyl chains stuck up over the water surface, the thickness of LB monolayer having the parallel arrangement of anhydroglucose unit is supposed to be about 2.9 nm, whereas the thickness of the monolayer having the vertical arrangement is calculated as 3.4 nm. As mentioned above, both AFM and X-ray reflection provided similar values with 3.7 ± 0.2 and 3.6 nm, respectively. Thus, the 23C18 LB monolayer can be assumed to possibly possess the vertical arrangement of anhydroglucose units as shown in Figure 7B.

(28) Zhang, Y.; Tun, Z.; Ritcey, A. M. *Langmuir* **2004**, *20*, 6187.

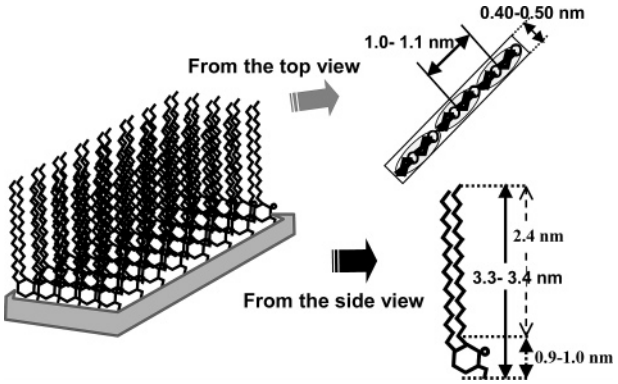

Figure 11. Molecular model of 23C18 LB monolayer.

However, the limiting molecular area of 23C18 prior to the compression was 55 Å^2 per anhydroglucose unit as already described. From this value, it is assumed that the LB monolayer of 23C18 before the compression was composed in the parallel arrangements of glucose ring planes as shown in Figure 7A. Namely, the arrangement of an anhydroglucose unit may be changed during the compression of the area of the monolayers, because hydroxyl groups remaining at the C-6 position of 23C18 may enhance hydrophilicity. Therefore, the arrangement may be differentiating from the initial arrangement suggested by the result of the limiting molecular area. A schematic image of the molecular side chain arrangements of 23C18 was then depicted in Figure 11. In general, a cellulose molecular chain owns the 2_1 screw axis. However, the above results indicate interestingly that the space group of the compressed LB monolayer of 23C18 may be in the 1_1 screw axis. With compression of the monolayer, the monolayer suprastructure would be strongly affected by a lack of intra- and/or intermolecular hydrogen bonds and more affected by hydrophobic interaction of the long alkyl chains. Therefore, conformation of the 2_1 screw of cellulose backbone may be facilitated to be changed into the unusual $\phi-\phi$ dihedral angle such as 1-fold axis without a symmetry element with increasing the surface pressure. Considering the side chain arrangements, we will add more detailed evidence in a future paper.

4. Conclusion

Regioselectively substituted cellulose ethers having long alkyl chains were used because of difficultly of purification due to physical entanglements between cellulose derivatives and residual C18 alkylation reagent. However, use of an isothermal crystallization procedure as the purification step in this study has solved this difficulty, and amphiphilic cellulose ethers were synthesized successfully.

Then, the LB monolayer of each derivative was fabricated on the water surface using a moving wall technique and then used for the analyses of the formation using several methods. Both $\pi-A$ isotherms and surface topography of each LB monolayer were completely different for the synthesized three cellulose ethers, resulting in the difference in physical properties such as solubility. This was considered to be due to the regioselective effect in the distribution of the alkyl group. The compressed 23C18 LB monolayer exhibited the most homogeneous surface of the three samples. The thickness of the LB monolayer was measured by two methods using X-ray reflection and AFM height mode. Both results were identical to be ca. 3.6 nm. This value indicates that the compressed 23C18 LB monolayer may be in a vertical arrangement with an up-ordering of the alkyl side chains on the individual glucose ring facing each other over the water surface, which is unusual in cellulose and the derivatives. Thus, conformation of the 2_1 screw of the cellulose backbone may be changed into an unusual conformation with a unique $\phi-\psi$ dihedral angle such as 1-fold axis without a symmetry element with increase in the surface pressure.

These results suggest that the formation of such compressed monolayers from regioselectively substituted cellulose ethers with long alkyl side chains were strongly influenced by the hydrophobic interaction among the distribution of long alkyl chains in the anhydroglucose unit and lack of inter- and/or intramolecular hydrogen bonds engaged in cellulose ethers. It also indicates that a certain compression force may even cause change in the twist of the cellulose backbone chain from a 2_1 screw.

Acknowledgment. We greatly thank Mr. T. Mitsunaga and Ms. A. Takase of the X-ray Diffraction Group, Application Laboratory, Rigaku Corporation for advise on X-ray diffractometer techniques. This research was supported in part by the Core Research for Evolutional Science and Technology (CREST) project of the Japan Science and Technology Agency (JST) in Japan and by a Grant-in-Aid for Scientific Research (No. 14360101), Japan Society for the Promotion of Science (JSPS).

LA047323J